

Research Article

Three Possible Encapsulation Mechanics of TiO₂ Nanoparticles into Single-Walled Carbon Nanotubes

Wisit Sukchom,^{1,2} Kittisak Chayantrakom,^{1,2}
Pairote Satiracoo,^{1,2} and Duangkamon Baowan^{1,2}

¹ Department of Mathematics, Faculty of Science, Mahidol University, Rama 6 Road Bangkok 10400, Thailand

² Centre of Excellence in Mathematics, CHE, Si Ayutthaya Road Bangkok 10400, Thailand

Correspondence should be addressed to Duangkamon Baowan, scdbw@mahidol.ac.th

Received 7 February 2011; Accepted 3 May 2011

Academic Editor: Shaogang Hao

Copyright © 2011 Wisit Sukchom et al. This is an open access article distributed under the Creative Commons Attribution License, which permits unrestricted use, distribution, and reproduction in any medium, provided the original work is properly cited.

Titanium dioxide nanoparticle (TiO₂-NP) is widely used in manufactured nanomaterials such as sunscreens, cosmetics, drugs, and some food products. It can be encapsulated in a single-walled carbon nanotube (SWNT) depending on their physical and chemical interactions. On applying the Lennard-Jones potential function and the continuous approximation, we determine three encapsulation mechanisms for spherical shape TiO₂-NP entering a tube: (i) head-on at the tube open end, (ii) around the edge of the tube open end, and (iii) through a defect opening on the tube wall. The total potential energy of the system is obtained as an exact expression by performing double surface integrals. We find that the TiO₂-NP is most (least) likely to be encapsulated into a SWNT by head-on configuration (around the edge of the tube open end). This encapsulation procedure is a potential application for targeted drug delivery. For convenience, throughout this analysis all configurations are assumed to be in vacuum and the TiO₂-NP is initially at rest.

1. Introduction

The unique chemical, physical, and electronic properties of single-walled carbon nanotubes (SWNTs) provide the most promising avenue of research into the fabrication of nanoscale one-dimensional systems [1, 2]. Self-assembled molecules in the SWNT's hollow core are expected to exhibit new features differing from those of the bulk materials [3, 4]. "Peapods," SWNTs filled with fullerenes [5, 6], are already exciting interest with future developments hopefully leading to composite materials fulfilling particular electronic or mechanical functions. However, the formation mechanisms regarding nanopeapods are currently uncertain. Suggestions about their unique behaviour have focused on the van der Waals interaction and the large surface area to volume of nanoparticles.

Titanium dioxide (TiO₂, titania) has been the subject of a number of studies in the fields of water and air purification, photocatalytic sterilisation of food and the environmental industry. The activity of TiO₂ against a wide variety of organisms, bacteria, algae, virus, and cancer cells, has been

reported. As a photocatalyst, the production of superoxide (O₂^{•-}) and hydroxyl radicals (•OH) due to absorption of light with a wavelength less than 385 nm (ultraviolet A, UV-A) occurs. This is due to the generation of electron-hole pairs which migrate to the surface in combination with a competition of trapping and recombination events in the body of lattice [7, 8]. Most studies suggest that hydroxyl radicals, which are able to oxidise organic substances and disrupt bacteria and virus, are the main cause of the bactericidal effect during photocatalysis [9, 10]. TiO₂ has been well studied because of its low price and abundance, its stability and nontoxicity, as well as its high oxidative power. The major drawback of TiO₂ is that its band gap occurs in the near-UV of the electromagnetic spectrum.

Combining TiO₂ with carbon nanotube as hybrid materials offers many important potential applications. We comment that there are other types of nanoparticles, such as gold and magnetic Fe₃O₄, that can be used to study these three encapsulation mechanics, here the TiO₂ molecule is employed as an example, and once an analytic expression is obtained it can be adapted to the other systems. In this paper,

utilising a simple model based on algebraic calculations using the Lennard-Jones potential as the force field, we investigate the feasibility of encapsulating TiO_2 in SWNT. The potential energy, force distribution, encapsulation energy, and consequent results for the assumed spherical TiO_2 particles are presented. Further, we employ the continuous approach where the atoms at discrete locations on the molecules are smeared over surfaces of a spherical nanoparticle and a cylindrical SWNT, as a result some electronic properties, metallic and semiconducting, of nanotubes are neglected, and only the radius of the tube is taken into account. In this paper, we consider only the potential energy of the system where the electrostatic potential between two molecules will be included in authors' future work.

The paper is organised as follows; the potential function and the continuous approximation of TiO_2 -SWNT systems are described in Section 2. In Section 3, we determine the three encapsulation mechanisms and their numerical results. Finally, conclusions are presented in Section 4. Using this model, we believe that many novel nanoscaled applications of these two particles will become apparent, possibly impacting on therapeutic research and the construction of nanoscale drug delivery systems.

2. Potential Energy and Force Distribution

The continuous approach has been utilised by many applicants to determine the interaction energy between two carbon nanostructures [11–17]. We have assumed that the carbon atoms on the nanotube and the titanium and oxygen on the TiO_2 are uniformly distributed over the surfaces of the two molecules, so that the continuous approximation can be used. It is in a form of double surface integrals, averaged over the surfaces of each entity, and we may deduce

$$U = \eta_1 \eta_2 \iint \Phi(\rho) dS_1 dS_2, \quad (1)$$

where η_1 and η_2 are the mean atomic surface densities of TiO_2 and carbon nanotube, respectively, and dS_1 and dS_2 are two surface elements. $\Phi(\rho)$ is a potential function between two atoms on each molecule, and ρ is a distance between two surface elements. In this study, the well-known Lennard-Jones potential function [18] is employed which is given by

$$\Phi(\rho) = -\frac{A}{\rho^6} + \frac{B}{\rho^{12}}, \quad (2)$$

where A and B are the attractive and repulsive constants, respectively. The resultant axial force in the z -direction is calculated by differentiating the potential energy with respect to Z , so that the force is obtained by

$$F_Z = -\frac{\partial U}{\partial Z}, \quad (3)$$

where Z is the distance from the tube open end to the centre of the TiO_2 molecule.

The suction energy or the encapsulation energy (W) is defined as the total energy or work done generated by van

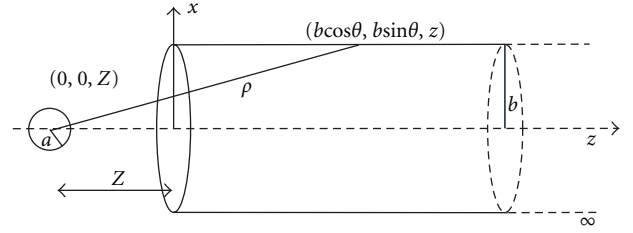


FIGURE 1: TiO_2 encapsulated into a carbon nanotube head-on at the tube open end.

der Waals interaction acquired by a particular molecule as a consequence of being sucked into the nanotube [11], and it can be written as

$$W = \int_{-\infty}^{\infty} F(Z) dZ = - \int_{-\infty}^{\infty} \frac{dU}{dZ} dZ = U(-\infty) - U(\infty), \quad (4)$$

which is transformed into kinetic energy. We note that the particle begins to enter into the tube when the suction energy is equal to zero.

3. Three Possible Encapsulation Mechanics

3.1. Encapsulation of TiO_2 Head-On at the Tube Open End. In this model, a TiO_2 molecule is assumed to be a sphere. Firstly, the energy and the force distribution for the TiO_2 molecule encapsulated into a single-walled carbon nanotube by entering the tube head-on at the tube open end are determined. After that, the maximum interaction energy can be determined by optimising the value of nanotube radius using the suction energy. This system is shown in Figure 1.

With reference to a rectangular Cartesian coordinate system (x, y, z) with origin located at the tube end, a typical point on the surface of the tube has the coordinates $(b \cos \theta, b \sin \theta, z)$ where b is the radius of the semi-infinite tube. Similarly, with reference to the same rectangular Cartesian coordinate system (x, y, z) , the centre of the TiO_2 molecule has coordinates $(0, 0, Z)$ where Z is the distance from the tube end to the centre of the TiO_2 molecule in the z -direction which can be either positive or negative. The radius of the spherical TiO_2 molecule is denoted by a . Thus the distance ρ between the centre of the TiO_2 and a typical point on the tube is given by

$$\rho^2 = b^2 + (z - Z)^2. \quad (5)$$

Firstly, we determine the interaction energy between a point and a spherical TiO_2 which is given by

$$U^*(\rho) = \frac{\pi a \eta_1}{\rho} \left[\frac{A}{2} \left(\frac{1}{(\rho + a)^4} - \frac{1}{(\rho - a)^4} \right) - \frac{B}{5} \left(\frac{1}{(\rho + a)^{10}} - \frac{1}{(\rho - a)^{10}} \right) \right], \quad (6)$$

where η_1 denotes the mean surface density of TiO_2 molecule. We note that the derivation for the above equation can be found in [11].

Using the Lennard-Jones potential function and the continuous approximation for a cylindrical carbon nanotube, the total potential energy can be obtained and it can be written as

$$U = \pi ab\eta_1\eta_2 \times \int_{-\pi}^{\pi} \int_0^{\infty} \frac{1}{\rho} \left[\frac{A}{2} \left(\frac{1}{(\rho+a)^4} - \frac{1}{(\rho-a)^4} \right) - \frac{B}{5} \left(\frac{1}{(\rho+a)^{10}} - \frac{1}{(\rho-a)^{10}} \right) \right] dzd\theta, \quad (7)$$

where η_2 represents the mean atomic surface density of carbon nanotube. The mean atomic surface density of TiO₂ is calculated from a single unit cell of the anatase structure, which is the most common mineral form of TiO₂ whereas the others are rutile and brookite. It is a tetragonal configuration with two TiO₂ units per a primitive cell and we may deduce $\eta_1 = 0.07498 \text{ \AA}^{-2}$ [19]. In the case of a carbon nanotube, it can be thought as a graphene sheet rolled up to form a cylinder, therefore we can simplify the mean atomic surface density of the tube from the graphene sheet, and we may deduce $\eta_2 = 0.3812 \text{ \AA}^{-2}$. Moreover, (7) can be rewritten as

$$U = 4\pi a^2 b \eta_1 \eta_2 \times \int_{-\pi}^{\pi} \int_0^{\infty} \left[-A \left(\frac{1}{(\rho^2 - a^2)^3} + \frac{2a^2}{(\rho^2 - a^2)^4} \right) + \frac{B}{5} \left(\frac{5}{(\rho^2 - a^2)^6} + \frac{80a^2}{(\rho^2 - a^2)^7} + \frac{336a^4}{(\rho^2 - a^2)^8} + \frac{512a^6}{(\rho^2 - a^2)^9} + \frac{256a^8}{(\rho^2 - a^2)^{10}} \right) \right] dzd\theta. \quad (8)$$

There is one form of the integral which needs to be evaluated, and it is defined by

$$G_n = \int_{-\pi}^{\pi} \int_0^{\infty} \frac{1}{(\rho^2 - a^2)^n} dzd\theta. \quad (9)$$

The derivation for G_n can be found in Baowan et al. [16], where we may deduce

$$G_n = \frac{2\pi}{(b^2 - a^2)^{n-1/2}} \int_{-\tan^{-1}[Z/(b^2 - a^2)]}^{\pi/2} \cos^{2(n-1)} \psi d\psi \quad (10)$$

and

$$\int \cos^{2(n-1)} \psi d\psi = \frac{1}{2^{2(n-1)}} \left[\binom{2(n-1)}{(n-1)} \psi + \sum_{k=0}^{n-2} \binom{2(n-1)}{k} \frac{\sin[(2n-2k-2)\psi]}{(n-k-1)} \right], \quad (11)$$

TABLE 1: Lennard-Jones constants used in this model.

Interaction	ϵ (meV)	σ (Å)	A (eV \times Å ⁶)	B (eV \times Å ¹²)
C-Ti	3.14	3.7588	35.38	9979.40
C-O	4.14	3.2531	19.61	23241.81
Graphene-Graphene	3.83	2.39	15.2	24100

where $\binom{n}{m}$ is the binomial coefficient. By evaluating (11) at $\psi = \pi/2$ and $\psi = -\tan^{-1}[Z/(b^2 - a^2)]$ an analytical expression for G_n may be obtained.

For the interaction between the TiO₂ molecule and the carbon nanotube, there are two different interactions which are C-Ti and C-O interactions. By their atomic proportion, the total potential energy can be determined as

$$U^{\text{Tot}} = \frac{1}{3} U(A_{\text{C-Ti}}, B_{\text{C-Ti}}) + \frac{2}{3} U(A_{\text{C-O}}, B_{\text{C-O}}). \quad (12)$$

The Lennard-Jones constants A and B for this system are given in Table 1 while the constants for C, Ti, and O are taken from the work of Mayo et al. [20] and the constants for graphene are taken from the work of Girifalco et al. [21].

The potential energy of the system depends on the distances in the z -directions. We illustrate graphically an example of the potential energy versus the distance Z for encapsulating a TiO₂ molecule with radius $a = 10 \text{ \AA}$ into carbon nanotubes with radii $b = 12.7$ and 13.5 \AA . In fact, the TiO₂ molecule will enter into the tube if the energy level inside the tube is lower than that outside the tube. From Figure 2(a), it is clearly seen that the TiO₂ will be encapsulated into the tube with radius 13.5 \AA . However, this phenomenon will not occur for the tube with radius 12.7 \AA . In the sense of force distribution as shown in Figure 2(b), the TiO₂ will enter into the tube if the force is positive which is in agreement with the result from energy behaviour.

The relation between the suction energy and the radius of nanotube b is shown in Figure 3 with three different values of TiO₂ radii a . For the case of $a = 10 \text{ \AA}$, the suction energy is zero when $b = b_0 = 12.7875 \text{ \AA}$ which is the tube radius at which the TiO₂ molecule begins to enter into the tube and the encapsulation process occurs when $b > b_0$. The maximum suction energy is 3.4187 eV , it occurs when the tube radius $b = 13.3039 \text{ \AA}$ which gives the radius difference as $b - a = 3.3039 \text{ \AA}$. These values are similar to those in the work of Baowan et al. [17].

Further, we observe similar behaviours for the cases of $a = 12$ and $a = 14 \text{ \AA}$ as illustrated in Figure 3. The maximum suction occurs at $b = 15.2994$ and 17.3024 \AA for $a = 12$ and 14 \AA , respectively, with corresponding to $b - a = 3.2994$ and 3.3024 \AA . Therefore, we may conclude that the maximum suction energy is insensitive to the variation of their radii, and it depends on the different of their radii. However, the change of the TiO₂ length has an effect on the third and fourth decimal places of this value, $b - a$.

3.2. Encapsulation of TiO₂ around the Edge of an Open End. In this model, the energy and the force distributions for a TiO₂ molecule encapsulated into a single-walled carbon nanotube by entering the tube around the edge of an open

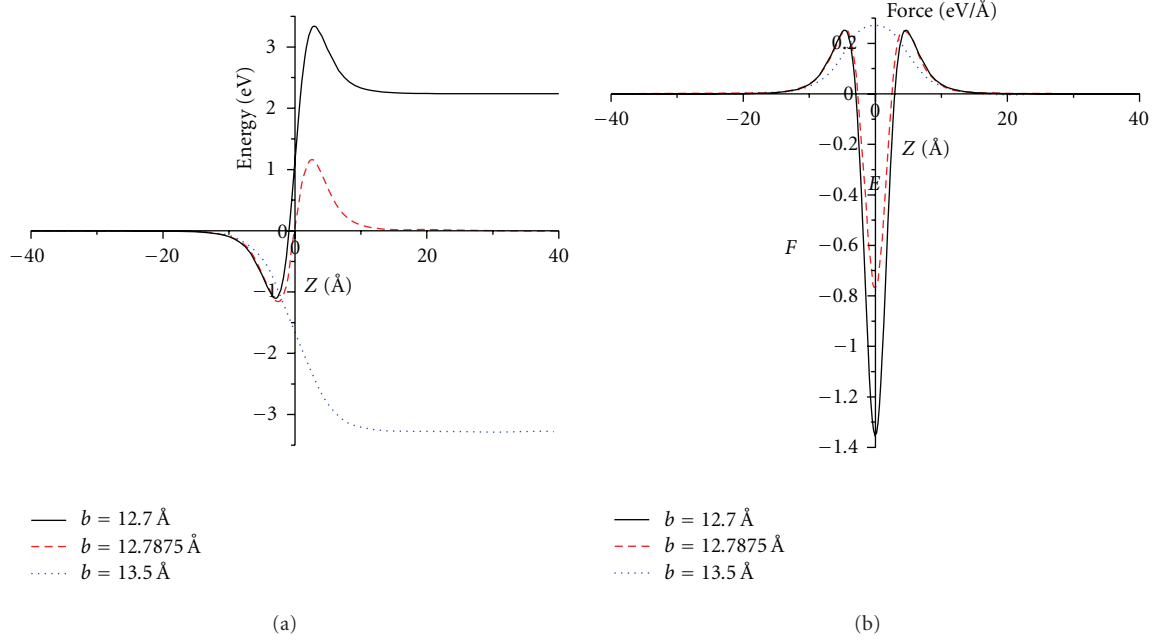


FIGURE 2: (a) Potential energy and (b) force distributions for TiO_2 with radius $a = 10 \text{ \AA}$ encapsulated into a carbon nanotube head-on at the tube open end.

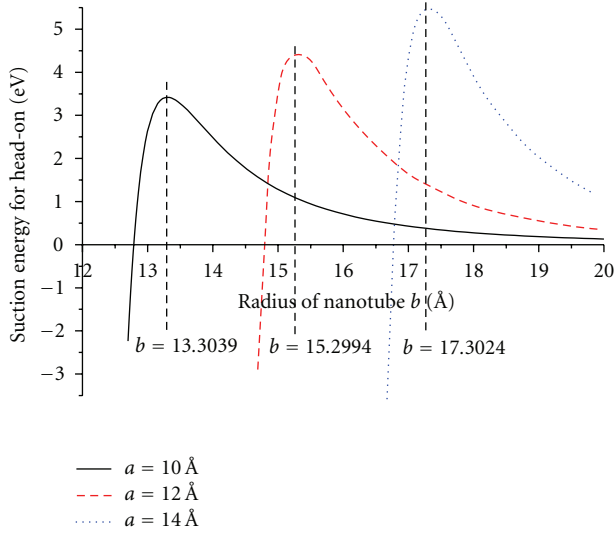


FIGURE 3: Suction energy for head-on configuration with three different nanoparticle radii $a = 10, 12, 14 \text{ \AA}$.

end are investigated. A schematic of this system is shown in Figure 4.

Again, with reference to a rectangular Cartesian coordinate system (x, y, z) with origin located at the tube end, a typical point on the surface of the tube has the coordinates $(b \cos \theta, b \sin \theta, z)$ where b is the radius of the semi-infinite tube. Similarly, with reference to the same rectangular Cartesian coordinate system (x, y, z) , the centre of the TiO_2 molecule has coordinates $(x, 0, Z)$ where Z is the distance in the z -direction which can be either positive or negative and x is the distance of the TiO_2 molecule in the x -direction. Thus

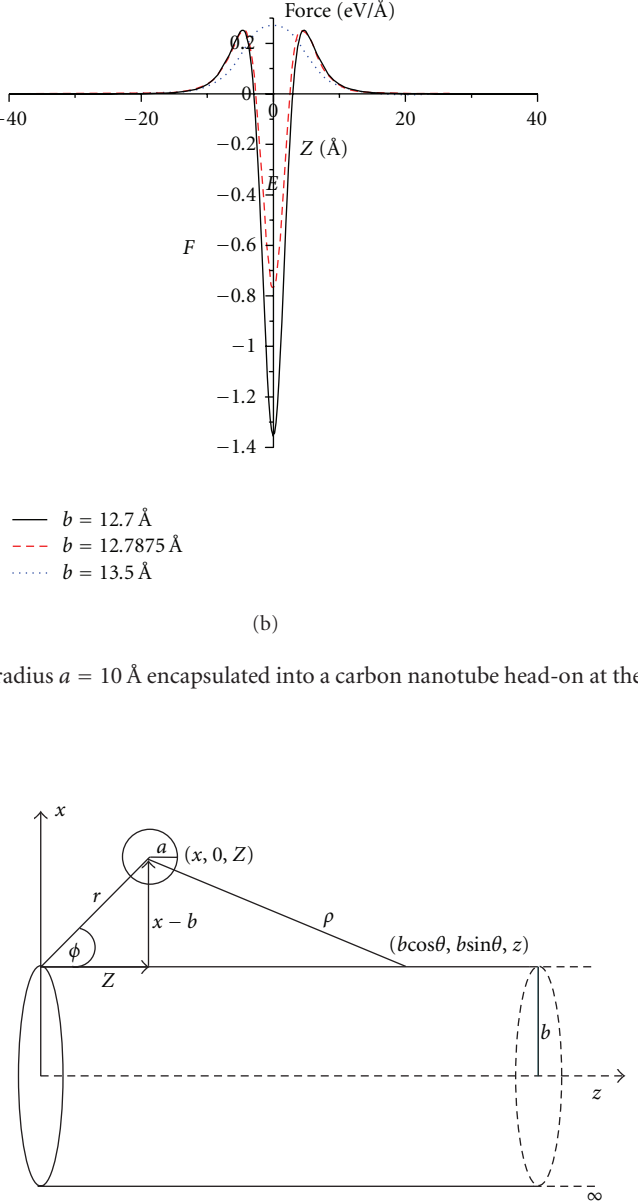


FIGURE 4: TiO_2 encapsulated into a carbon nanotube around the edge of the tube open end.

the distance ρ between the centre of the TiO_2 molecule and a typical point on the tube is given by

$$\begin{aligned} \rho^2 &= (b \cos \theta - x)^2 + b^2 \sin^2 \theta + (z - Z)^2 \\ &= (b - x)^2 + 4bx \sin^2 \left(\frac{\theta}{2} \right) + (z - Z)^2. \end{aligned} \quad (13)$$

Using the Lennard-Jones potential function and the continuous approximation, the total potential energy can be written as (7) where ρ is given by (13). Furthermore, there is another

form of the integral which needs to be evaluated, where we define as

$$H_n = \int_{-\pi}^{\pi} \int_0^{\infty} \frac{1}{(\rho^2 - a^2)^n} dz d\theta. \quad (14)$$

We note that in the case of (14), ρ is a function of two variables which are Z and x . Further, an analytical expression for (14) consists of three parts in terms of the standard hypergeometric function, which are presented in the work of Baowan et al. [16].

In Figure 5(a), we illustrate graphically an example of the potential energy versus the distances x and Z for encapsulating the TiO_2 molecule with radius $a = 10 \text{ \AA}$ into carbon nanotubes with radii $b = 12.7$ and 13.5 \AA . Firstly, we consider the potential energy level, it is obvious that the potential energy is higher than in the former case so that in this case the TiO_2 molecule has less likely chance to encapsulate in the carbon nanotube.

In the case of $b = 12.7 \text{ \AA}$ as shown in Figure 5(a), the suction energy is zero when $x = x_0 = 25.2267 \text{ \AA}$ and we obtain $\Delta x_0 = b - x_0 = 2.5267 \text{ \AA}$. The maximum suction energy, 0.39501 eV , occurs at $x = 25.7284 \text{ \AA}$ which gives $\Delta x_{\max} = 3.0284 \text{ \AA}$, and the TiO_2 molecule will not be sucked into the carbon nanotube if the distance x is greater than 45.2398 \AA . We note that the distance x has to be greater than $a + b$ for the TiO_2 molecule to be located above outside the tube.

Similarly for $b = 13.5 \text{ \AA}$ as shown in Figure 5(b), the suction energy is zero when $x = x_0 = 26.0270 \text{ \AA}$. Moreover, we obtain $\Delta x_0 = 2.5270 \text{ \AA}$ which is the distance in the x direction between the surface of the TiO_2 molecule and the tube wall. The maximum suction energy, 0.40058 eV , occurs at $x = 26.5288 \text{ \AA}$ which gives $\Delta x_{\max} = 3.0288 \text{ \AA}$. If the distance x is greater than 46.1589 \AA , the TiO_2 molecule will not be sucked into the carbon nanotube since the global minimum energy is located farther along the tube in the positive z -direction.

Next, we consider only the positive z -direction where the TiO_2 molecule is located above the tube. In this case, the TiO_2 will not be encapsulated into the tube if its position is far away from the tube open end. The reason is that the energy at this point is lower than the energy barrier near the tube end. However, a nanopeapod can be formed if we give an initial energy to the TiO_2 molecule to be greater than the energy barrier. Moreover, if the TiO_2 molecule is initiated at rest closer to the tube open end, it has a higher probability of being encapsulated around the tube edge.

3.3. Encapsulation of TiO_2 at a Defect Opening on the Tube Wall. In this model, we investigate the potential energy for a TiO_2 molecule encapsulated into a carbon nanotube at a defect opening on the tube wall, where the centre of TiO_2 is located midway along the tube length. Since the Lennard-Jones potential is only effective at short range, the carbon nanotube is assumed to be infinite in length. The total potential energy of this case is calculated by subtracting the total energy of the TiO_2 interacting with the defect pad from

the total potential energy of the TiO_2 interacting with the infinite nanotube, as shown in Figure 6.

Again, with reference to a rectangular Cartesian coordinate system (x, y, z) with origin located at the centre of the tube, a typical point on the surface of the tube has the coordinates $(b \cos \theta, b \sin \theta, z)$ where b is the radius of the infinite tube. Similarly, with reference to the same rectangular Cartesian coordinate system (x, y, z) , the centre of the TiO_2 molecule has coordinates $(x, 0, Z)$ where Z is the distance in the z -direction which can be either positive or negative and x is the distance of the TiO_2 molecule in the x -direction. Thus the distance ρ between the centre of the TiO_2 and a typical point on the tube is given by

$$\begin{aligned} \rho^2 &= (b \cos \theta - x)^2 + b^2 \sin^2 \theta + (z - Z)^2 \\ &= (b - x)^2 + 4bx \sin^2 \left(\frac{\theta}{2}\right) + (z - Z)^2. \end{aligned} \quad (15)$$

On letting

$$\begin{aligned} \Phi^*(\rho) &= \frac{1}{\rho} \left[\frac{A}{2} \left(\frac{1}{(\rho + a)^4} - \frac{1}{(\rho - a)^4} \right) \right. \\ &\quad \left. - \frac{B}{5} \left(\frac{1}{(\rho + a)^{10}} - \frac{1}{(\rho - a)^{10}} \right) \right], \end{aligned} \quad (16)$$

the total potential energy of the TiO_2 interacting with the infinite nanotube is given by

$$U_{\text{tube}} = \pi ab \eta_1 \eta_2 \int_{-\pi}^{\pi} \int_{-\infty}^{\infty} \Phi^*(\rho) dz d\theta. \quad (17)$$

The defect pad is assumed to be in the region where $Z \in (-L, L)$ and $\theta \in (-\theta_0, \theta_0)$ so that the total energy of the TiO_2 interacting with the defect pad is given by

$$U_{\text{pad}} = \pi ab \eta_1 \eta_2 \int_{-\theta_0}^{\theta_0} \int_{-L}^L \Phi^*(\rho) dz d\theta. \quad (18)$$

The defect pad is arbitrarily chosen as a square with the length L , which is determined from the summation of the radius a of the TiO_2 and the equilibrium interspacing between the TiO_2 and the nanotube which is 3.304 \AA [17]. Utilising the arc length formula $S = r\theta$ where S is the arc length, r is the radius of the circle, and θ is the angle in radians made by the arc at the centre of the circle, the limit of the integration, θ_0 , is adopted to be settled from $L = b\theta_0$. Note that there is only a minor effect on the energy profile when we vary θ_0 , and the overall properties of the system remain the same when L is greater than the critical value 13.304 \AA .

Thus the total potential energy for the TiO_2 encapsulated in the carbon nanotube at the defect opening on the tube wall is obtained by

$$\begin{aligned} U &= \pi ab \eta_1 \eta_2 \left(\int_{-\pi}^{\pi} \int_{-\infty}^{\infty} \Phi^*(\rho) dz d\theta \right. \\ &\quad \left. - \int_{-\theta_0}^{\theta_0} \int_{-L}^L \Phi^*(\rho) dz d\theta \right). \end{aligned} \quad (19)$$

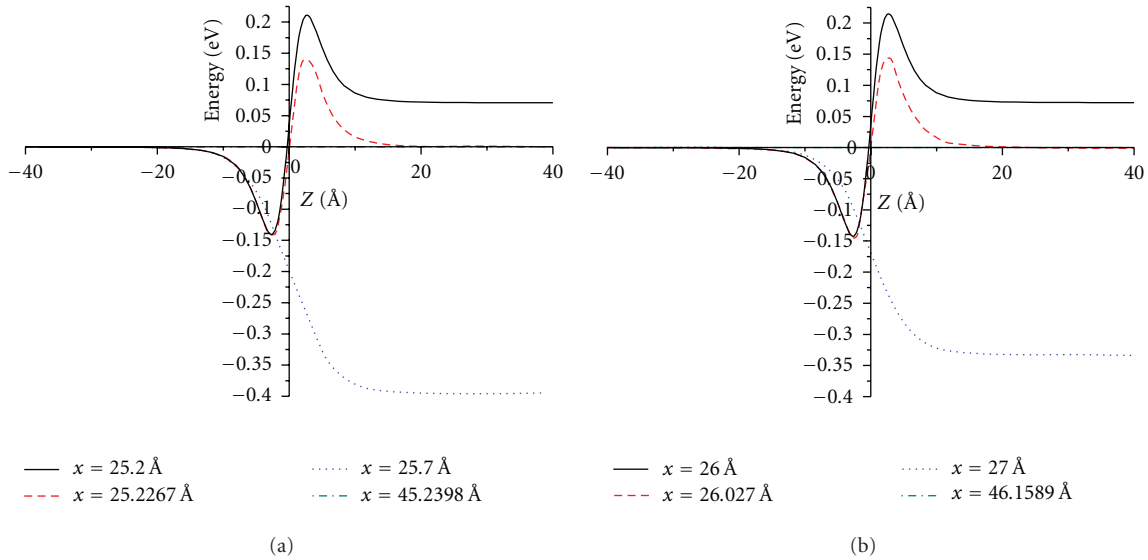


FIGURE 5: Potential energy for TiO_2 with radius $a = 10 \text{ \AA}$ encapsulated into carbon nanotubes with radius (a) $b = 12.7 \text{ \AA}$ and (b) $b = 13.5 \text{ \AA}$ around the edge of the tube open end where the distance x is fixed.

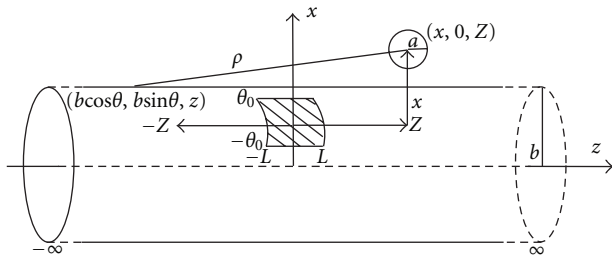


FIGURE 6: TiO_2 encapsulated into a carbon nanotube at defect opening on the tube wall.

By using precisely the same analytical method as shown in the previous section, we separately determine the energy for the tube and that for the pad, and numerically calculate the total potential energy for the system.

We examine the relation between the potential energy and the distance Z for the different values of x which are the interspacing between the TiO_2 molecule and the carbon nanotube surface. The behaviours of all cases are similar. Two examples of the potential energy versus the distances x and Z for encapsulating the TiO_2 molecule with radius $a = 10 \text{ \AA}$ into a carbon nanotube with radii $b = 12.7$ and 13.5 \AA are shown in Figure 7. We consider the interaction energy at both edges of the defect pad because the point force singularity is affected from the edges and we get an approximate value at 0.2 eV . We observe that there are two potential energy peaks near the edges of the defect pad when $x \leq 25.7288$ and $x \leq 26.5288 \text{ \AA}$ for $b = 12.7$ and 13.5 \AA , respectively. Therefore, an initial energy is required for the TiO_2 molecule to be encapsulated into the carbon nanotube if the TiO_2 molecule is located outside the region of the defect pad. However, the TiO_2 is spontaneously sucked through the defect pad when its position is directly above the defect pad.

Furthermore, the TiO_2 molecule will not be sucked through the defect pad to form a nanopapod if the value of x is greater than 25.7288 and 26.5288 \AA for $b = 12.7$ and 13.5 \AA , respectively, because the position of the global minimum energy is located farther from the defect pad along the carbon nanotube in the z -direction.

4. Conclusions

In this paper, we investigate a nanopapod which is a well-known self-assembled hybrid carbon nanostructure comprising a TiO_2 molecule and a carbon nanotube. We consider three encapsulation site scenarios for the TiO_2 molecule entering the carbon nanotube which are (i) head-on at the tube open end, (ii) around the edge of the tube open end, and (iii) through a defect opening on the tube wall. The TiO_2 is assumed to be initially at rest prior to enter into the two specific carbon nanotubes which are 12.7 \AA and 13.5 \AA in radius in a vacuum environment. We utilise the classical Lennard-Jones potential function and the continuous approximation to determine the potential energy which may be expressed in terms of the hypergeometric function. Because of the complicated analytical expressions, we use the algebraic computer package MAPLE to perform numerical evaluations.

In Figure 8, we compare the potential energy and encapsulation energy for the three encapsulation mechanisms. It is found that the TiO_2 molecule is most likely to enter the carbon nanotube head-on at the tube open end. The reason is that the overall attractive force arises from the entire tube, and this mechanism avoids the point force singularity acting at the edge of the tube. Encapsulation at a defect pad is the second most likely mechanism to form the nanopapod. There is an effect from the edges of the defect pad but the TiO_2 molecule is sucked into the tube if

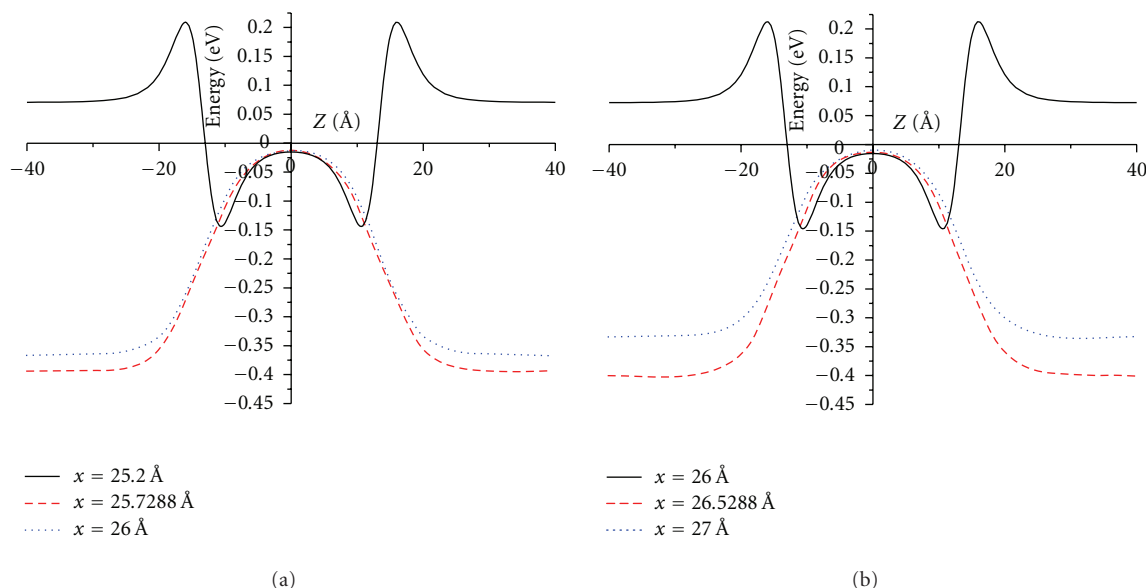


FIGURE 7: Potential energy for TiO_2 with radius $a = 10 \text{ \AA}$ encapsulated into a carbon nanotube with radius (a) $b = 12.7 \text{ \AA}$ and (b) $b = 13.5 \text{ \AA}$ at defect opening on the tube wall where the distance x is fixed.

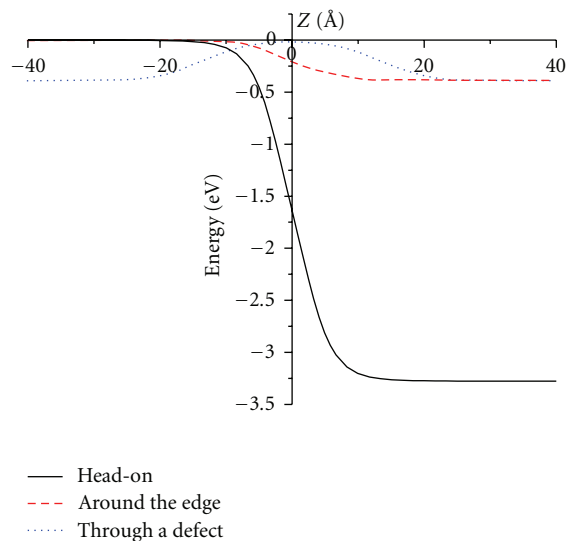


FIGURE 8: Potential energy for TiO_2 with radius $a = 10 \text{ \AA}$ encapsulated into a carbon nanotube with radius $b = 13.5 \text{ \AA}$ and $x = 26.4 \text{ \AA}$ for the three encapsulation mechanisms.

its location is directly above the defect pad. The least feasible mechanism to encapsulate the TiO_2 molecule into the tube is entering around the edge of the tube open end because the TiO_2 molecule must overcome the strong repulsive forces at the tube extremities and change its direction of motion as moving into the tube. Although these results might be as expected, this theoretical study is a first step in understanding the complex system for the encapsulation of drug molecules into a nanocapsule.

In comparison to other methods used to study nanoscience and nanotechnology, such as first principle calculations, molecular dynamics, or Monte Carlo simulations,

our applied mathematical modelling approach are not been widely used in this field. However, mathematical modelling can generate important insights into complex processes and reveal optimal parameters or situations that might be otherwise almost impossible through experimentation.

Acknowledgment

This paper is funded by the Centre of Excellence in Mathematics, Thailand, and this financial support is gratefully acknowledged.

References

- [1] S. Iijima and T. Ichihashi, "Single-shell carbon nanotubes of 1-nm diameter," *Nature*, vol. 363, no. 6430, pp. 603–605, 1993.
- [2] D. S. Bethune, C. H. Kiang, M. S. De Vries et al., "Cobalt-catalysed growth of carbon nanotubes with single-atomic-layer walls," *Nature*, vol. 363, no. 6430, pp. 605–607, 1993.
- [3] M. M. Calbi, M. W. Cole, S. M. Gatica, M. J. Bojan, and G. Stan, "Colloquium: condensed phases of gases inside nanotube bundles," *Reviews of Modern Physics*, vol. 73, no. 4, pp. 857–865, 2001.
- [4] A. N. Khlobystov, D. A. Britz, A. Ardavan, and G. A. D. Briggs, "Observation of ordered phases of fullerenes in carbon nanotubes," *Physical Review Letters*, vol. 92, no. 24, Article ID 245507, 3 pages, 2004.
- [5] B. W. Smith, M. Monthieux, and D. E. Luzzi, "Encapsulated C_{60} in carbon nanotubes," *Nature*, vol. 396, no. 6709, pp. 323–324, 1998.
- [6] S. Okada, S. Saito, and A. Oshiyama, "Energetics and electronic structures of encapsulated C_{60} in a carbon nanotube," *Physical Review Letters*, vol. 86, no. 17, pp. 3835–3838, 2001.
- [7] A. V. Emeline, A. V. Frolov, V. K. Ryabchuk, and N. Serpone, "Spectral dependencies of the quantum yield of photochemical processes on the surface of nano/micro-particulates of

wide-band-gap metal oxides. IV. Theoretical modeling of the activity and selectivity of semiconductor photocatalysts with inclusion of a subsurface electric field in the space charge region," *Journal of Physical Chemistry B*, vol. 107, no. 29, pp. 7109–7119, 2003.

- [8] N. Serpone, *The KirkOthmer Encyclopedia of Chemical Technology*, John Wiley & Sons, New York, NY, USA, 2000.
- [9] J. C. Ireland, P. Klostermann, E. W. Rice, and R. Clark, "Inactivation of escherichia coli by titanium dioxide photocatalytic reaction," *Applied and Environmental Microbiology*, vol. 59, pp. 1668–1670, 1993.
- [10] M. Cho, H. Chung, W. Choi, and J. Yoon, "Different inactivation behaviors of MS-2 phage and Escherichia coli in TiO₂ photocatalytic disinfection," *Applied and Environmental Microbiology*, vol. 71, no. 1, pp. 270–275, 2005.
- [11] B. J. Cox, N. Thamwattana, and J. M. Hill, "Mechanics of atoms and fullerenes in single-walled carbon nanotubes. II. Oscillatory behaviour," *Proceedings of the Royal Society A*, vol. 463, no. 2078, pp. 477–494, 2007.
- [12] B. J. Cox, T. A. Hilder, D. Baowan, N. Thamwattana, and J. M. Hill, "Continuum modelling of gigahertz nano-oscillators," *International Journal of Nanotechnology*, vol. 5, no. 2-3, pp. 195–217, 2008.
- [13] T. A. Hilder and J. M. Hill, "Oscillating carbon nanotubes along carbon nanotubes," *Physical Review B*, vol. 75, no. 12, Article ID 125415, 2007.
- [14] D. Baowan, N. Thamwattana, and J. M. Hill, "Suction energy and offset configuration for double-walled carbon nanotubes," *Communications in Nonlinear Science and Numerical Simulation*, vol. 13, no. 7, pp. 1431–1447, 2008.
- [15] D. Baowan and J. M. Hill, "Suction energy and oscillatory behavior for carbon nanocones," *Journal of Computational and Theoretical Nanoscience*, vol. 5, pp. 302–310, 2008.
- [16] D. Baowan, N. Thamwattana, and J. M. Hill, "Encapsulation of C₆₀ fullerenes into single-walled carbon nanotubes: fundamental mechanical principles and conventional applied mathematical modeling," *Physical Review B*, vol. 76, no. 15, Article ID 155411, 8 pages, 2007.
- [17] D. Baowan, W. Triampo, and D. Triampo, "Encapsulation of TiO₂ nanoparticles into single-walled carbon nanotubes," *New Journal of Physics*, vol. 11, Article ID 093011, 2009.
- [18] J. E. Lennard-Jones, "Cohesion," *Proceedings of the Physical Society*, vol. 43, no. 5, pp. 461–482, 1931.
- [19] A. Fahmi, C. Minot, B. Silvi, and M. Causa, "Encapsulation of TiO₂ nanoparticles into single walled carbon nanotubes," *Physical Review Letters*, vol. 47, pp. 11717–11724, 1993.
- [20] S. L. Mayo, B. D. Olafson, and W. A. Goddard III, "DREIDING: a generic force field for molecular simulations," *Journal of Physical Chemistry*, vol. 94, no. 26, pp. 8897–8909, 1990.
- [21] L. A. Girifalco, M. Hodak, and R. S. Lee, "Carbon nanotubes, buckyballs, ropes, and a universal graphitic potential," *Physical Review B*, vol. 62, no. 19, pp. 13104–13110, 2000.



Hindawi

Submit your manuscripts at
<http://www.hindawi.com>

